

Single-frequency fibre laser with a cavity formed by Bragg gratings written in the core of an active composite fibre using KrF laser radiation (248 nm)

O.N. Egorova, O.I. Medvedkov, E.S. Seregin, S.A. Vasil'ev, S.E. Sverchkov, B.I. Galagan, B.I. Denker, G.L. Danielyan, V.I. Pustovoi, S.L. Semjonov

Abstract. The possibility of producing a single-frequency fibre laser using a new type of fibre made by sintering phosphate glass in a silica glass tube (composite fibre) is demonstrated. In a fibre of this type, photosensitivity to laser radiation with a wavelength of 248 nm is detected. A fibre laser cavity is fabricated by writing fibre Bragg gratings directly in the core of the composite optical fibre activated by erbium ions. Stable single-frequency linearly polarised lasing regime is obtained at a wavelength of 1559.5 nm with a maximum output power of ~3 mW.

Keywords: single-frequency fibre laser, composite optical fibre, photosensitivity, fibre Bragg gratings.

1. Introduction

Despite the fact that single-frequency fibre lasers have been a subject of research and development for several decades, interest in this topic has not diminished [1, 2]. Significant progress in the development of single-frequency fibre lasers has been achieved using optical fibres entirely consisting of phosphate glass [3], since it allows the introduction of rare-earth ions with a high concentration. High concentrations of active rare-earth elements make it possible to obtain a high gain per unit length, which is important when making single-frequency fibre lasers, the operation of which requires a small cavity length.

The possibility of obtaining high generation efficiency with a rather short length of a new type of active fibre – a composite fibre made by sintering phosphate glass in a silica glass tube – was shown in [4–7]. Despite the fact that in the process of drawing such fibres, the phosphate and silica glasses cross-diffuse, because of which the composition of the glass in the core changes significantly, the concentrations of phosphorus oxide and active rare-earth ions in the core are still much higher than in fibres usually produced by silica glass vapour deposition. The high concentration of active

rare-earth ions in such fibres allows the development of single-frequency fibre lasers based on them. Owing to the silica glass cladding, these optical fibres are preferable to optical fibres entirely consisting of phosphate glass. They are more resistant to environmental influences, they are easier to connect to silica optical fibres, and the resulting junctions are reliable due to the absence of differences in physicochemical properties (unlike junctions of optical fibres made of different glasses).

In Ref. [8], we showed the possibility of manufacturing a single-frequency fibre laser, the cavity of which is formed by fibre Bragg gratings written directly in the core of an active composite fibre by radiation at a wavelength of 193 nm (ArF laser). However, the question arises: is it possible to inscribe Bragg gratings using irradiation at a wavelength of 248 nm (KrF laser)? This excimer laser is the most convenient one and, therefore, it is the main actual tool for writing Bragg gratings in optical fibres. KrF lasers are significantly more reliable, easier to operate, and their working mixture has a much longer life compared to ArF lasers. In the present work, it was shown that the available photosensitivity of a composite fibre to radiation at a wavelength of 248 nm (KrF laser) allows the formation of a cavity of a single-frequency fibre laser. Using a composite fibre activated with erbium ions, a single-frequency fibre laser was manufactured operating at a wavelength of 1559.5 nm in a stable single-frequency linearly polarised regime.

2. Optical fibre

The studied fibre was fabricated by sintering phosphate glass in a silica glass tube with subsequent drawing of an optical fibre [5, 8]. For the core to be manufactured, glass of the same composition as in [5–7] was used. This composition contained 65 mol% P₂O₅, 7 mol% Al₂O₃, 12 mol% B₂O₃, 9 mol% Li₂O and 7 mol% Re₂O₃ [9]. The concentration of erbium ions was $1.0 \times 10^{20} \text{ cm}^{-3}$ (1.1 wt.% or 0.39 mol.% of erbium oxide). The composition of the glass also included gadolinium, with the total concentration of rare-earth ions being about 7 mol.%. To fabricate a fibre from bulk phosphate glass, a cylinder with a diameter of about 4 mm was drilled using a hollow diamond drill, then the cylinder was inserted into a silica glass tube and the assembly was sintered at a temperature of 2000 °C in the furnace of the fibre-optic fibre-drawing machine. After redrawing the resulting preform into rods with a diameter of 1 mm and jacketing an additional silica glass tube, the optical fibre was drawn.

The diameter of the core of the manufactured fibre, estimated using a photograph of the end of the fibre obtained by

O.N. Egorova, S.E. Sverchkov, B.I. Galagan, B.I. Denker, G.L. Danielyan, V.I. Pustovoi Prokhorov General Physics Institute, Russian Academy of Sciences, ul. Vavilova 38, 119333 Moscow, Russia; e-mail: egorova@nsc.gpi.ru;
O.I. Medvedkov, S.A. Vasil'ev, S.L. Semjonov Fiber Optics Research Center, Russian Academy of Sciences, ul. Vavilova 38, 119333 Moscow, Russia;
E.S. Seregin FORC-Photonics, korpus 3, Nauchnyi proezd 20, 117246 Moscow, Russia

Received 15 October 2019
Kvantovaya Elektronika 49 (12) 1112–1116 (2019)
Translated by V.L. Derbov

means of an electron microscope, was approximately $4.5\ \mu\text{m}$. The diameter of the silica glass cladding was $125\ \mu\text{m}$.

As noted in our earlier papers, during the drawing of a fibre with a phosphate glass core and a silica cladding, significant mutual diffusion of phosphate and silica glasses occurs. To determine the degree of mutual diffusion in the obtained fibre, the concentration of phosphorus oxide in the core was estimated by X-ray microanalysis using a JSM-5910 LV scanning electron microscope (JEOL) and an INCA X-ray spectrometer (Oxford Instruments). The electron beam was directed to the centre of the fibre core, while the electron energy was selected so that the diameter of the X-ray generation region was about $3.5\ \mu\text{m}$, i.e., smaller than the diameter of the core. According to estimates, the concentration of phosphorus oxide in the core was about 24 mol.%. To assess the concentration of aluminum, lithium, boron, and gadolinium oxides that make up the initial glass, we assumed that it decreases proportionally to the decrease in the concentration of phosphorus oxide in the core of the fibre compared to the original glass.

The mode composition of the obtained fibre at wavelengths near $1.55\ \mu\text{m}$ was studied by observing the end image using an IR camera. Under different excitation conditions, only the intensity distribution corresponding to the fundamental mode of the fibre core was observed at the output end of the fibre under study. This indicates that the fabricated fibre was single-mode in the near $1.55\ \mu\text{m}$. Using a fibre 2 m long, the cut-off wavelength of the first highest mode, which was measured by the bend reference technique, was $1.4\ \mu\text{m}$.

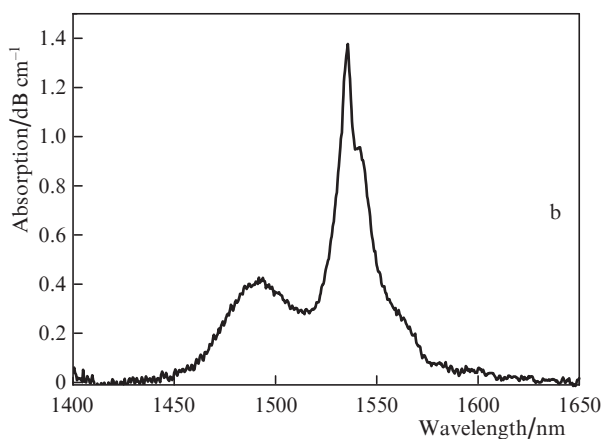
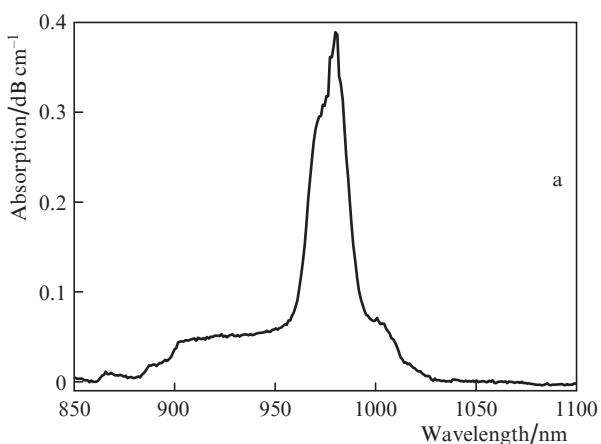


Figure 1. Absorption spectra of the composite fibre near the wavelengths of (a) 0.98 and (b) $1.55\ \mu\text{m}$.

Figure 1 shows the absorption spectra of the obtained fibre near 980 and $1550\ \text{nm}$ in the small-signal regime. The maximum absorption at a wavelength of $980\ \text{nm}$ is approximately $0.4\ \text{dB cm}^{-1}$. Figure 2 shows the luminescence spectrum measured upon excitation at a wavelength of $980\ \text{nm}$. The measured lifetime of the energy level ${}^4I_{13/2}$ of erbium ions was $6.1\ \text{ms}$. Such a small value of the lifetime compared with that characteristic of optical fibres made by the deposition of silica glass from the gas phase is obviously due to the significant content of hydroxyl groups in the initial phosphate glass.

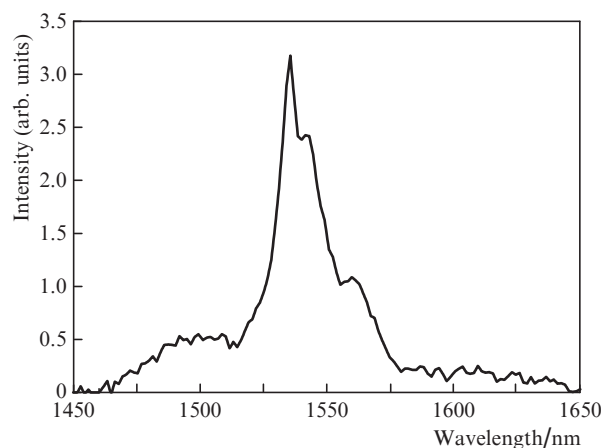


Figure 2. Luminescence spectrum of a composite fibre.

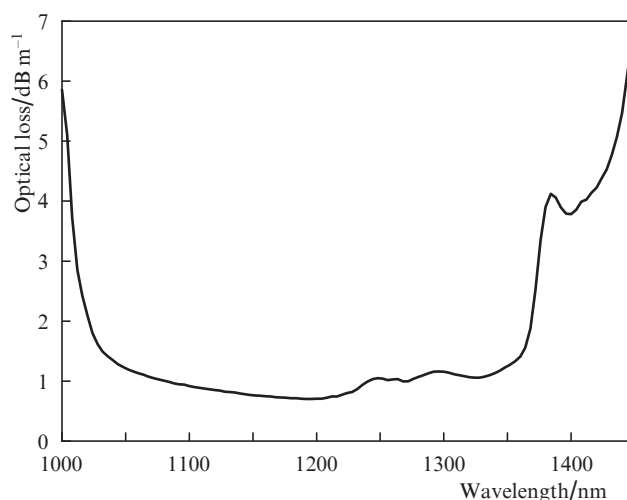


Figure 3. Spectrum of optical loss.

Figure 3 shows the spectrum of optical losses beyond the absorption bands of erbium ions, measured by shortening the fibre length. The minimum optical loss in this region is $1\ \text{dB m}^{-1}$ and is determined mainly by the degree of contamination of phosphate glass during melting [10].

3. Laser

To form the laser cavity, fibre Bragg gratings were written directly in the active composite fibre. The gratings were written by radiation from a CL-5000 excimer KrF laser ($248\ \text{nm}$) (OptoSystems) through a uniform phase mask with a period $\Lambda_m = 1072.03\ \text{nm}$ and a length of $50\ \text{mm}$. To increase photosensitivity, the active composite fibre was loaded with

molecular hydrogen at a temperature of 100°C and a pressure of 110 atm. KrF laser radiation (pulse duration 10 ns, energy 24 mJ, repetition rate 50 Hz) was focused by a cylindrical lens onto the side surface of the fibre through a phase mask.

Initially, the possibility of writing Bragg gratings directly in the core of a composite fibre was experimentally investigated. For this purpose, under the conditions described above, a Bragg grating of 3.5 mm length was written. During the writing, the transmission spectra of the fibre were measured at various doses of UV radiation. The measurements were carried out using an ANDO 6317B spectrum analyser with a resolution of 0.02 nm and a broadband luminescent source. Using the obtained dynamics of the reflection coefficient of the Bragg grating and applying the technique from [11], we calculated the dependence of the induced change in the refractive index on the dose of UV radiation (Fig. 4). Comparison of this dependence with similar data for the standard SMF28e telecommunication fibre, studied under conditions close to the conditions of the present experiment [12], showed that the induced refractive index is comparable for two types of optical fibres at doses of UV irradiation of less than 4 kJ cm⁻². At UV irradiation doses above 4 kJ cm⁻² in the composite fibre under study, the growth rate of the induced refractive index slows down significantly, while this does not occur in the SMF28e fibre. Nevertheless, a change in the refractive index at the level of $(4-6) \times 10^{-4}$ induced in the core of the composite fibre is sufficient to form a cavity of a single-frequency fibre laser.

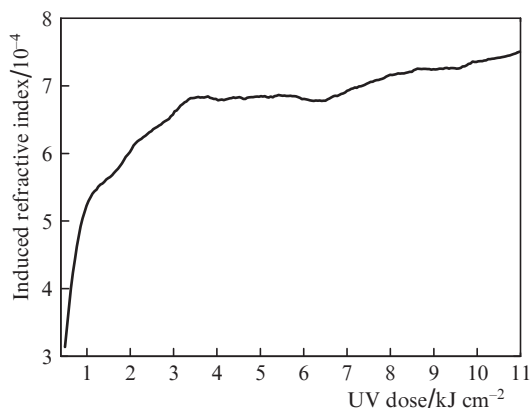


Figure 4. Dependence of the induced refractive index in a composite optical fibre on the UV radiation dose.

The laser cavity was formed by two identical fibre Bragg gratings 23 mm long each. Between the gratings there was a portion of an unirradiated active fibre with a length of 4 mm. The cavity was written by scanning the UV laser beam along the axis of the fibre at a speed of 0.05 mm s⁻¹ in two passes. After each pass, the transmission spectrum of the cavity was measured. The reflection coefficient of the gratings after the first pass was approximately 90%.

The final transmission spectrum of the cavity, formed by two gratings, is shown in Fig. 5. The reflection coefficient of each grating is about 98%; the width of the spectrum at half maximum is 0.16 nm. Since the studied pair of gratings is a Fabry–Perot interferometer with a high Q factor, a narrow peak is present in the spectrum corresponding to the trans-

mission band of the interferometer. Based on the geometric parameters of the cavity and the measured reflection coefficient of the gratings, we can estimate the spectral width of the central transmission peak in the reflection spectrum of the Fabry–Perot interferometer [11]. According to the calculations, the spectral peak width at half-maximum $\Delta\lambda$ (FWHM) is 0.003 nm. The obtained value is less than the maximum resolution of the used spectral device (0.01 nm); therefore, this peak in Fig. 5 cannot be resolved.

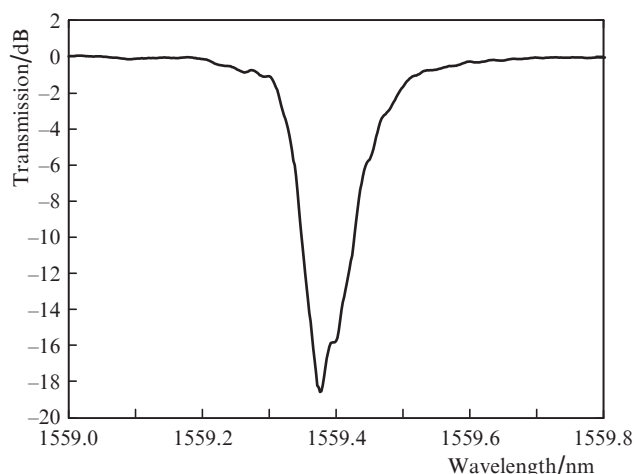


Figure 5. Transmission spectrum of the laser cavity, measured with a resolution of 0.01 nm.

Based on the parameters of the obtained cavity, it is possible to estimate the wavelength difference of the adjacent longitudinal modes of the cavity [13]. With a grating length of 23 mm, a distance between gratings of 4 mm and a reflection coefficient of gratings of 98%, the calculated wavelength difference between adjacent longitudinal cavity modes is 0.065 nm (8 GHz). It should be noted that, in numerical estimates, the grating parameters were assumed the same. However, due to temperature changes during the writing of the gratings, their real parameters may differ.

Figure 6 schematically shows the setup for studying the characteristics of the obtained fibre laser. A semiconductor laser diode with a wavelength of 976 nm was used as a source of pump radiation. The total length of the active fibre was approximately 70 mm: 50 mm per cavity, and 10 mm on each side of the cavity were necessary to connect the latter with the rest of the circuit. An active fibre was spliced on both sides to a specially manufactured fibre doped with germanium oxide. The diameters of the mode fields of the germanium and active fibres almost coincided and amounted to about 5 μ m at a wavelength of 1550 nm.

The mode composition of the obtained laser operating in a stable single-frequency regime was studied using a confocal scanning Fabry–Perot interferometer with a free dispersion region of 750 MHz. Due to the presence of a small birefringence in the cavity inherent in the active fibre, the laser operated in the regime with two orthogonal polarisations of radiation (Fig. 7a). The orthogonality of the mode polarisations was determined using the polarisation controller installed at the output of the system and a polariser located in front of the entrance to the Fabry–Perot scanning interferometer. By bending the active fibre in a certain direction, it was possible to obtain a stable single-frequency regime with linear polarisation.

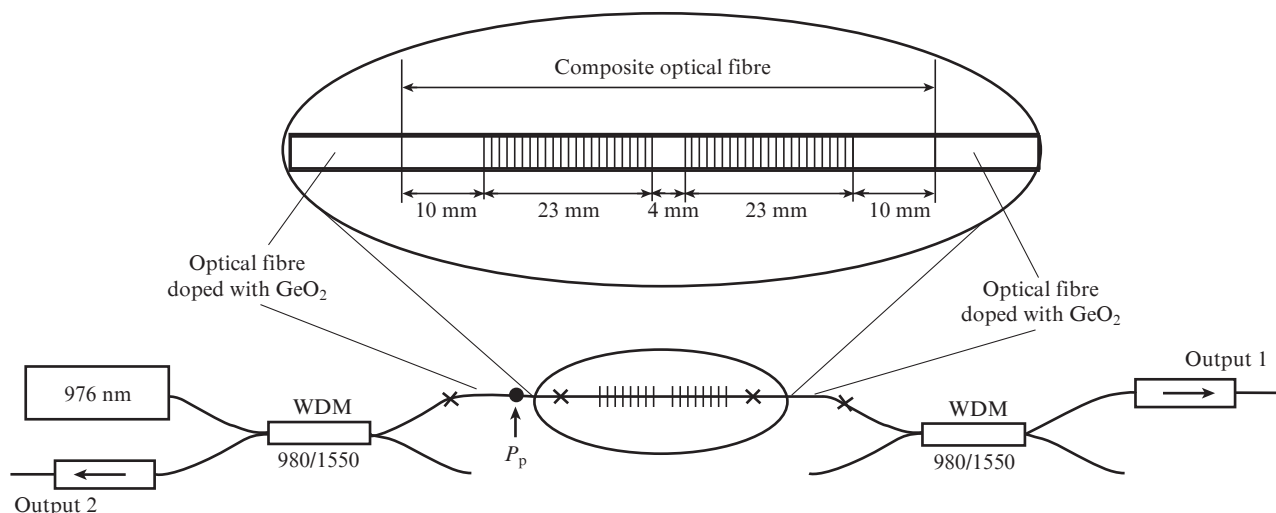


Figure 6. Schematic of the setup for studying the characteristics of a fibre laser.

sation (Fig. 7b). Apparently, the bending of the optical fibre led to an increase in birefringence inside the cavity and, consequently, to an increase in the frequency difference between the orthogonally polarised modes. The width of the lasing line, measured using a Fabry–Perot scanning interferometer,

was smaller than the instrumental width of the interferometer (11 MHz).

A study of the temporal characteristics of a laser using a photodetector with a bandwidth of 2 GHz and an oscilloscope (500 MHz) showed the absence of pulsing. At a pump power in the range of 90–320 mW (measured at the point P_p in Fig. 6), the laser signal was Fourier-transformed. The peak frequency of relaxation oscillations increased from 220 to 650 kHz with an increase in the pump power from 90 to 320 mW. No other noise frequency components were detected.

The laser emission spectrum, measured at pump powers of about 89, 183, and 320 mW with a resolution of 0.01 nm, is shown in Fig. 8. At the highest power, the lasing wavelength was 1559.5 nm. The change in the laser radiation wavelength with increasing pump power is due to the heating of the Bragg gratings.

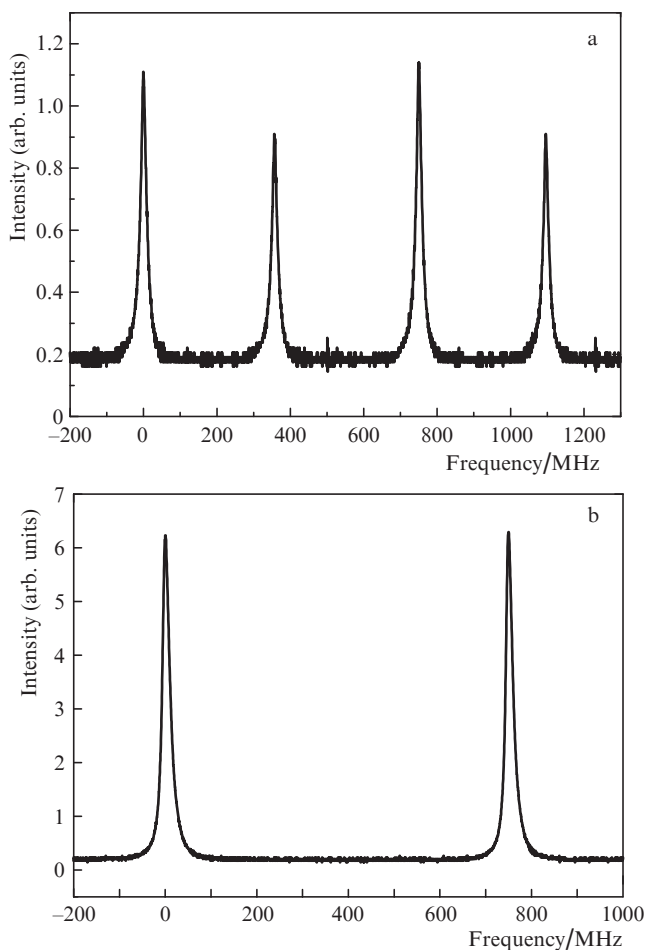


Figure 7. Laser modes recorded using a Fabry–Perot scanning interferometer with a free dispersion region of 750 MHz in the case of (a) two polarisations and (b) one polarisation.

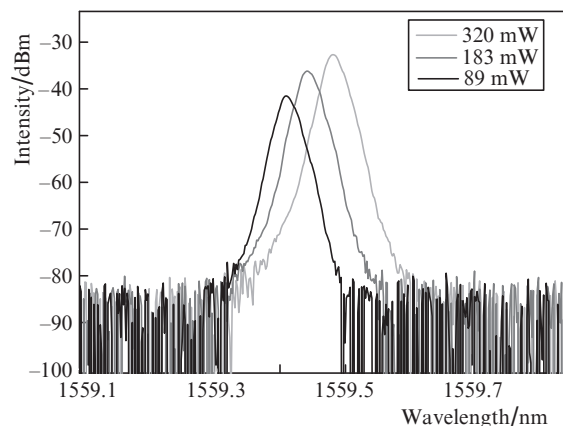


Figure 8. Laser emission spectra at various pump powers.

Figure 9 shows the dependences of the laser power output from both sides (output 1 and output 2, Fig. 6) on the input pump power, measured in a linearly polarised laser oscillation regime (with bending). The oscillation threshold is about 70 mW. The launched pump power was measured at point P_p . The unabsorbed pump power at output 1 was about a third of the input, and the lasing efficiency was 1.2%. The laser power

at output 2 was approximately half that of output 1. This is obviously due to the difference in the reflection coefficients of the gratings making up the laser cavity, or to their slight mismatch in wavelength.

The bent of the laser cavity was implemented by fixing the germanium-doped fibre sections on the laboratory bench (see Fig. 6) without using any special devices. A change in the position of the active fibre significantly affected the output power and the state of polarisation of the laser radiation. Thus, the amplitude of the output power oscillations when the spatial position of the fibre laser cavity was changed exceeded 50%. However, at a certain position of the fibre, it was possible to obtain laser generation in a linearly polarised mode with a sufficiently stable output power (within 5%) in time, which was sufficient for measurements. In this case, the lasing efficiency approximately corresponded to the dependence shown in Fig. 9.

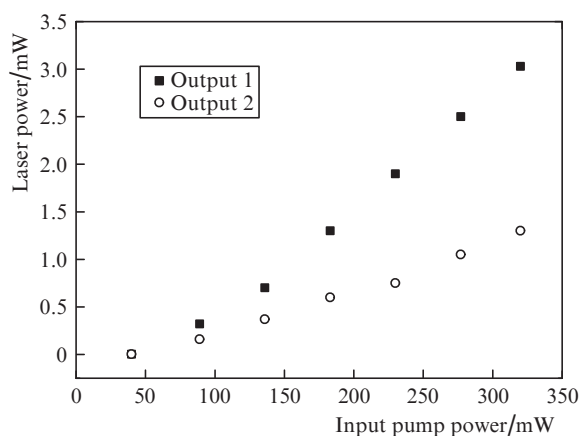


Figure 9. Dependence of the laser output power on the input pump power.

4. Conclusions

The possibility of writing fibre Bragg gratings in a composite optical fibre manufactured by sintering a phosphate glass in a silica glass tube using the radiation of a KrF laser at a wavelength of 248 nm is demonstrated. For this purpose, a composite fibre doped with erbium ions, single-mode near a wavelength of 1550 nm, was designed and manufactured. In hydrogen-loaded samples of a composite fibre, photosensitivity to laser radiation with a wavelength of 248 nm was found, comparable with the photosensitivity of a hydrogen-loaded standard telecommunication fibre with a core made of germanosilicate glass. When writing Bragg gratings directly in the core of an active composite fibre, the operation of a single-frequency laser was demonstrated. The fabricated fibre laser generated radiation at a wavelength of 1559.5 nm in a stable single-frequency linearly polarised mode.

Acknowledgements. The authors are grateful to the staff of the FORC-Photonics for their help in manufacturing fibre Bragg gratings.

References

1. Yang Z., Li C., Xu S., Yang C. *Single-Frequency Fiber Lasers* (Singapore: Springer, 2019).
2. Shi W., Fang Q., Zhu X., Norwood R.A., Peyghambarian N. *Appl. Opt.*, **53**, 6554 (2014).
3. Fu S., Shi W., Feng Y., Zhang L., Yang Z., Xu S., Zhu X., Norwood R.A., Peyghambarian N. *J. Opt. Soc. Am. B*, **34**, A49 (2017).
4. Martin R.A., Knight J.C. *IEEE Photonics Technol. Lett.*, **18**, 574 (2006).
5. Egorova O.N., Galagan B.I., Denker B.I., Sverchkov S.E., Semenov S.L. *Quantum Electron.*, **46**, 1071 (2016) [*Kvantovaya Elektron.*, **46**, 1071 (2016)].
6. Egorova O.N., Semjonov S.L., Velmiskin V.V., Yatsenko Yu.P., Sverchkov S.E., Galagan B.I., Denker B.I., Dianov E.M. *Opt. Express*, **22**, 7632 (2014).
7. Egorova O.N., Semjonov S.L., Medvedkov O.I., Astapovich V.S., Okhrimchuk A.G., Galagan B.I., Denker B.I., Sverchkov S.E., Dianov E.M. *Opt. Lett.*, **40**, 3762 (2015).
8. Rybaltovsky A.A., Egorova O.N., Zhuravlev S.G., Galagan B.I., Denker B.I., Sverchkov S.E., Semjonov S.L. *Opt. Lett.*, **44**, 3518 (2019).
9. Karlsson G., Laurell F., Tellefsen J., Denker B., Galagan B., Osiko V., Sverchkov S. *Appl. Phys. B*, **75**, 41 (2002).
10. Galagan B.I., Glushchenko I.N., Denker B.I., Kalachev Yu.L., Mikhailov V.A., Sverchkov S.E. *Glass Phys. Chem.*, **37**, 258 (2011).
11. Othonos A., Kalli K. *Fiber Bragg Gratings: Fundamentals and Applications in Telecommunications and Sensing* (Norwood, Mass.: Artech House, 1999).
12. Swart P.L., Shlyagin M.G., Chtcherbakov A.A., Spirin V.V. *Electron. Lett.*, **38**, 1508 (2002).
13. Barmenkov Y.O., Zalvidea D., Torres-Peiró S., Cruz J.L., Andrés M.V. *Opt. Express*, **14**, 6394 (2006).